Differential Dynamic Behavior of Actin Filaments Containing Tightly-Bound Ca^{2+} or Mg^{2+} in the Presence of Myosin Heads Actively Hydrolyzing ATP†

Conrad A. Rebello and Richard D. Ludescher*

Department of Food Science, Rutgers, The State University, 65 Dudley Road, New Brunswick, New Jersey 08901-8520

Received February 12, 1999; Revised Manuscript Received August 9, 1999

ABSTRACT: We have investigated how Ca^{2+} or Mg^{2+} bound at the high-affinity cation binding site in F-actin modulates the dynamic response of these filaments to ATP hydrolysis by attached myosin head fragments (S1). Rotational motions of the filaments were monitored using steady-state phosphorescence emission anisotropy of the triplet probe erythrosin-5-iodoacetamide covalently attached to cysteine 374 of actin. The anisotropy of filaments containing only Ca^{2+} increased from 0.080 to 0.137 upon binding S1 in a rigor complex and decreased to 0.065 in the presence of ATP, indicating that S1 induced additional rotational motions in the filament during ATP hydrolysis. The comparable anisotropy values for Mg^{2+}-containing filaments were 0.067, 0.137, and 0.065, indicating that S1 hydrolysis did not induce measurable rotational motions in these filaments. Phalloidin, a fungal toxin which stabilizes F-actin and increases its rigidity, increased the anisotropy of F-actin containing either Ca^{2+} or Mg^{2+} but not the anisotropy of the 1:1 S1−actin complexes of these filaments. Mg^{2+}-containing filaments with phalloidin bound also displayed increased rotational motions during S1 ATP hydrolysis. A strong positive correlation between the phosphorescence anisotropy of F-actin under specific conditions and the extent of the rotational motions induced by S1 during ATP hydrolysis suggested that the long axis torsional rigidity of F-actin plays a crucial role in modulating the dynamic response of the filaments to ATP hydrolysis by S1. Cooperative responses of F-actin to dynamic perturbations induced by S1 during ATP hydrolysis may thus be physically mediated by the torsional rigidity of the filament.

F-Actin is a dynamically labile filament. Studies of filament formation going back to the early studies of Oosawa (*1*) have revealed the complexity of the monomer−filament equilibrium (*2, 3*). Subsequent research has, among other aspects, emphasized the dynamic role that filament-binding proteins such as gelsolin play in the cellular control of filament formation (*4*). Biophysical studies have also focused on the large-scale conformational dynamics of the filament and their relationship to monomer structure. Numerous studies of the large-scale filament dynamics using light scattering (*5*−*7*), fluorescence microscopic imaging of fluctuating filaments (*8*−*12*), dynamic rheology (*13*−*15*), and optical phosphorescence anisotropy (*16*−*21*) have animated the structural model of F-actin (*22, 23*). The anisotropic actin filament is now thought to exhibit two distinct modes of large-scale flexibility: long axis bending motions reflecting filament flexural rigidity and long axis twisting motions reflecting filament torsional rigidity. The biophysical details and functional implications of these two distinct motional modes are only now being actively evaluated.

Although F-actin does not appear to play a direct role in force generation per se, filament flexibility does appear to be important in contraction. Recent X-ray studies on muscle fibers (*24*) and on intact muscle (*25, 26*) have suggested that extensibility of the actin filament provides nearly half of the sarcomere compliance of an active muscle during isometric contraction. Wakabayashi et al. (*25*) have also observed that during isometric contraction there are slight changes in F-actin's helical structure including variations in the axial rise per residue of monomers as well as variations in the pitch of the genetic and long pitch helices.

By virtue of the helical organization of actin monomers in the filament, one would anticipate that these structural changes (helical rearrangements) manifest themselves in some manner as torsional motions within F-actin. These expectations are supported by various studies suggesting that myosin heads induce torsional twisting motions in F-actin during ATP hydrolysis. In vitro motility studies (*10, 27*) indicate that the vectorial motion of filaments driven by ATP hydrolysis in attached HMM involves a torsional twisting component, while solution studies of the rotational dynamics of actoS1[1] filaments by phosphorescence suggest that ATP hydrolysis induces rotational motions in F-actin in solution (*18*).

However, there is some controversy as to the cause of these additional twisting motions seen in F-actin during ATP

† This research was supported by a grant from the Muscular Dystrophy Association (to R.D.L.) and by a graduate assistantship (to C.A.R.) provided by the New Jersey Agricultural Experiment Station. This is publication number D-10567-2-99 of the New Jersey Agricultural Experiment Station.

* To whom correspondence should be addressed. Fax: 732-932-6776. Telephone: 732-932-9611, ext 231. E-mail: ludescher@aesop.rutgers.edu.

[1] Abbreviations: AMP-PNP, adenylyl imidodiphosphate; DTT, dithiothreitol; EGTA, ethylene glycol tetraacetic acid; EPPS, 4-(2-hydroxyethyl)-1-piperazineethanesulfonic acid; Er5IA, erythrosin-5-iodoacetamide; FB, filament buffer; F-Ca^{2+}-actin, F-actin polymerized with Ca^{2+} ion; F-Mg^{2+}-actin, F-actin polymerized with Mg^{2+} ion; F-(Mg^{2+}/Ca^{2+})-actin, F-actin polymerized with both Ca^{2+} and Mg^{2+} ions; GB, globular buffer; MOPS, 4-morpholinepropanesulfonic acid; S1, myosin subfragment 1.

10.1021/bi990348a CCC: $18.00
Published on Web 09/17/1999

hydrolysis. Nishizaka et al. (*10*) attributed the twisting motions observed in F-actin during ATP hydrolysis to torque applied by S1 to the filament. This interpretation was questioned by Suzuki et al. (*28*), who estimated that the rotational component of the sliding force applied by the attached myosin heads would amount to only about 10% of the total sliding force. Such a small twisting force may not bring about the torsional twisting motions observed in the actin filament during ATP hydrolysis. This view was supported by Yasuda et al. (*12*), who concluded from estimates of the magnitude of the sliding forces and actin's flexural and torsional rigidities that the actin filament would appear as an undeformable wire to a single myosin molecule.

An alternative interpretation of the twisting motions seen in F-actin during ATP hydrolysis (*29*) proposed that the rigor binding of myosin heads to F-actin may impose a constraint on the helical disorder that is inherently present in an actin filament. Upon release of this constraint during steady-state ATP hydrolysis, the actin filament would 'relax' from its strained state; no specific mechanism for this relaxation was advocated. Electron microscopy studies of F-actin (*44*) as a function of time following photoactivated release of caged adenylyl imidodiphosphate (AMP-PNP) indicating that nucleotide binding distorts the actin filament provide visual support for such a model. The relaxation of the actin filament from a torsionally strained state, however, would occur via torsional motions of monomers or groups of monomers in the filament. Large cooperative torsional motions in the actin filament should manifest themselves on the microsecond time scale.

We have recently provided evidence from steady-state phosphorescence anisotropy measurements (*21*) that the type of cation bound at the high-affinity binding site in the nucleotide cleft modulates the rotational motions of F-actin under a variety of conditions including the presence of phalloidin and the type of bound nucleotide (ATP or ADP). Measurements of the torsional rigidity of such Mg^{2+}- or Ca^{2+}-containing filaments (*12*) had suggested that the torsional rigidity is about 3-fold lower when Mg^{2+} is bound. These studies provide a new perspective on an ongoing controversy on the effect of divalent cations on the physical properties of F-actin. While Orlova and Egelman (*30, 31*) have interpreted the structural effects of divalent cation binding to F-actin in terms of the influence of cations on filament flexural rigidity, we suggest that the effects correlate better with changes in the torsional rigidity rather than in the flexural rigidity of the filament (*21*).

The present study examined the influence of tightly bound divalent cations on the ability of myosin to modulate the rotational motions of actin filaments in rigor and during active ATP hydrolysis. Rotational motions in F-actin were monitored using the steady-state phosphorescence emission anisotropy of a phosphorescent probe, erythrosin-5-iodoacteamide, covalently attached to Cys-374 of actin (*17, 18, 21, 32*), a technique which can provide an indirect measure (*33*) of the microsecond torsional flexibility of actin filaments (*16, 19, 20*). The current study demonstrated that the rotational motion of both Mg^{2+}- and Ca^{2+}-containing filaments decreased cooperatively upon binding myosin heads (S1) in the absence of ATP. However, ATP hydrolysis by attached myosin heads (S1) induced additional rotational motions in the more rigid Ca^{2+}-containing filaments, but not in the more flexible Mg^{2+}-containing filaments. Phalloidin binding increased the rigidity of both types of filaments, with the result that Mg^{2+}-containing filaments with phalloidin bound became sensitive to S1-induced rotations on the microsecond phosphorescence time scale. These results are interpreted in terms of differences in the cooperative response of the filament to torsional perturbations induced by S1 hydrolysis arising from the effects of divalent cation on the torsional rigidity of the filament.

MATERIALS AND METHODS

Protein Preparation and Labeling. Actin was isolated from acetone powder prepared from the leg and back muscles of New Zealand white rabbits of either sex (*34*). G-Actin was isolated from acetone powder by extraction into G-Buffer (GB: 1 mM EPPS, 0.2 mM $CaCl_2$, 1 mM NaN_3, 0.2 mM ATP, pH 8.5) containing 0.5 mM DTT as described in (*35*); such a procedure generates globular actin with Ca^{2+} at the high-affinity site (G-Ca^{2+}-actin). Actin was stored as filaments with continuous dialysis against filament buffer (FB: 10 mM MOPS, 100 mM KCl, 2 mM $MgCl_2$, 0.2 mM $CaCl_2$, 1 mM NaN_3, 0.2 mM ATP, pH 7.0) at 0 °C; the dialysis buffer was changed weekly. Actin concentration was determined by the absorbance at 290 nm using an extinction coefficient of 0.63 $(mg/mL)^{-1}$ cm^{-1} for actin. The protein was assayed for purity using SDS−PAGE. Actin was labeled with the phosphorescent probe erythrosin-5-iodoacetamide (Molecular Probes Inc., Eugene, OR) as per previously reported procedures (*32*) and was stored in the filament form by dialysis against FB on ice.

F-(Ca^{2+}/Mg^{2+})-actin (actin polymerized in the presence of both cations) was prepared by polymerizing G-actin with FB (*32*) and was dialyzed against this buffer. An actin filament containing predominantly Ca^{2+} at the high-affinity divalent cation binding site, F-Ca^{2+}-actin, was prepared by polymerizing G-Ca^{2+} with a modified filament buffer containing only calcium as the divalent cation (Ca^{2+}-FB: 10 mM MOPS, 100 mM KCl, 2.2 mM $CaCl_2$, 1 mM NaN_3, 0.2 mM ATP, pH 7.0) and was dialyzed against this buffer. G-Actin containing Mg^{2+} at the high-affinity divalent cation binding site (G-Mg^{2+}-actin) was prepared according to the protocol of Egelman and colleagues (*36*) by incubating G-Ca^{2+}-actin with 0.4 mM EGTA and 0.2 mM $MgCl_2$ for 10−15 min at 4 °C. G-Mg^{2+}-actin was then polymerized to F-Mg^{2+}-actin (actin filaments containing predominantly Mg^{2+} at the high-affinity divalent cation binding site) in a modified filament buffer (Mg^{2+}-FB: 10 mM MOPS, 100 mM KCl, 0.2 mM EGTA, 2.2 mM $MgCl_2$, 1 mM NaN_3, 0.2 mM ATP, pH 7.0).

Myosin was isolated from the leg and back muscles of New Zealand white rabbits. Myofibrils were prepared from this white muscle (*35*), and myosin was purified from the myofibrils (*18*). Subfragment 1 (S1) was prepared by proteolytic cleavage of myosin with α-chymotrypsin (*18*), and the isolated S1 was lyophilized in the presence of 0.1 M sucrose and stored at −20 °C. When required, a measured amount of lyophilized S1 was dialyzed against the appropriate filament buffer (FB, Ca^{2+}-FB, or Mg^{2+}-FB) containing 0.5 mM DTT. The S1 was assayed for purity using SDS−PAGE.

Spectroscopic Measurements. Steady-state fluorescence and light scattering measurements were made on a SPEX

model F1T11i spectrofluorometer (SPEX Industries, Metuchen, NJ) equipped with a 450 W high-pressure xenon lamp, single-grating excitation and emission monochromators, dual emission monochromators in a T-format, Glan−Thomson crystal polarizers on excitation and emission, and a circulating water bath to control the sample temperature. The instrument is under control of a microcomputer running DM3000F software (SPEX Industries). Phosphorescence measurements were made on this instrument equipped with a pulsed, low-pressure Xe flash lamp and a model 1934C phosphorimeter attachment (SPEX Industries).

Samples for spectroscopic measurements were prepared by mixing labeled and unlabeled actin to adjust the total concentration of erythrosin to 1 μM and the total concentration of actin (labeled and unlabeled) to 0.5 mg/mL. All luminescence measurements are done under anaerobic conditions using an enzymatic deoxygenation protocol (*37*). Steady-state fluorescence emission anisotropy spectra and steady-state phosphorescence emission anisotropy and intensity decay experiments were conducted according to previously reported protocols (*18*, *21*, *32*).

Determination of Relative Amounts of S1 Bound during ATP Hydrolysis. To determine the fraction of S1 bound to F-actin during ATP hydrolysis, various acto−S1 complexes were preincubated at 20 °C for 1 h in FB. An aliquot was withdrawn in order to determine the fraction of S1 bound to F-actin in rigor. To the remaining sample was added 25 mM ATP immediately prior to centrifugation (45 000 rpm for 50 min) in a Beckman L8-80 centrifuge at 4 °C. The supernatants were collected, and the resulting pellet was suspended in the original amount of FB. The original (uncentrifuged) samples, the supernatants obtained after centrifugation, and the suspended pellet were run on 7.5% SDS−PAGE gels. The intensities of the Coomassie blue R stained protein bands were then estimated by scanning the gels with a Molecular Dynamics Personal Densitometer SI, interfaced to a microcomputer running Image QuaNT Version 4.1 software.

Kinetic Measurements. Light scattering of a solution of erythrosin-labeled F-Mg^{2+}-actoS1 was used to monitor the release of S1 from actin followed by rebinding after ATP depletion. Light scattering was measured by emission at 425 nm using 425 nm excitation on the SPEX fluorometer. Light scattering from the rigor solution was measured for 600 s followed by addition of ATP to the solution and mixing (the curve is discontinuous because the fluorometer automatically closes a shutter to the emission detector while the sample compartment is open); a continuous time scan then followed the release and rebinding of S1. Scattering from an identical solution of pure F-actin under the same experimental conditions provided a measure of the signal from F-actin plus unbound S1 (which does not scatter significantly). Anisotropy as a function of time following addition of ATP was measured by defining the time for addition of ATP as time zero; the time of each measurement (which took approximately 5 min) was defined as the time when the data collection for vertical and horizontal was finished. There is thus considerable uncertainty in the time corresponding to each anisotropy measurement. Light scattering and anisotropy versus time curves were normalized to the same time scale by aligning the times for addition of ATP.

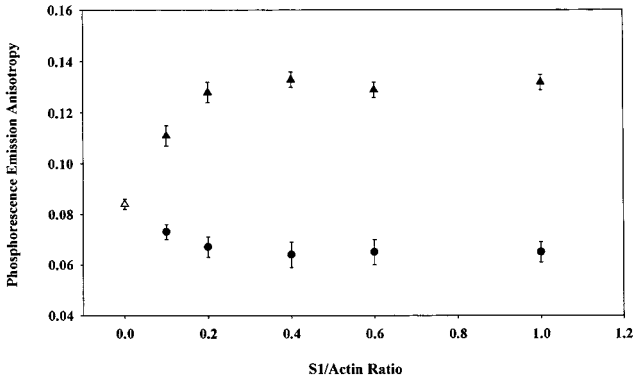

FIGURE 1: Steady-state phosphorescence emission anisotropy of F-(Ca^{2+}/Mg^{2+})-actin (△) and of 1:1 F-(Ca^{2+}/Mg^{2+})-actoS1 complexes in rigor (▲) and during steady-state ATP hydrolysis (●) in the presence of 25 mM ATP. All measurements were made at 20 °C in FB buffer containing 100 mM KCl.

RESULTS

Anisotropy of F-(Ca^{2+}/Mg^{2+})-ActoS1 Complexes in Rigor and during Steady-State ATP Hydrolysis. In a previous phosphorescence anisotropy study (*18*), we found that addition of ATP to an actoS1 complex polymerized in the presence of both Ca^{2+} and Mg^{2+} in buffer FB [F-(Ca^{2+}/Mg^{2+})-actin] caused a significant decrease in the phosphorescence anisotropy of F-actin at a stoichiometry of 1 S1 per actin. The time course of the anisotropy decrease coincided with the time calculated from the ATPase rate for complete ATP hydrolysis under the experimental conditions studied. Based on previous studies of torsional motions in actomyosin solutions (*10*, *27*) and an analysis of the types of motion detected by the phosphorescence polarization (see Discussion below), we suggested that these results indicated that S1 induced additional large-scale torsional motions in F-actin during ATP hydrolysis.

In Figure 1 we provide a more detailed investigation of the dynamic behavior of F-(Ca^{2+}/Mg^{2+})-actin in the absence and presence of ATP as a function of the S1:actin ratio. The steady-state phosphorescence emission anisotropy of erythrosin-labeled F-(Ca^{2+}/Mg^{2+})-actin was 0.086 ± 0.003 (Table 1). Upon titrating these filaments with S1 in the absence of ATP to form rigor complexes, the anisotropy increased nonlinearly from 0.086 (no S1) to 0.132 (1 S1 per actin). This increase in the anisotropy upon formation of a rigor complex is not due to trivial changes in probe properties such as lifetime (Table 1) upon binding S1, but rather reflects an overall decrease in the rotational motions of F-actin (*17*−*20*). During steady-state ATP hydrolysis, the anisotropy of the 1:1 actoS1 filament complex decreased from 0.132 to 0.065, a value significantly lower than the anisotropy of pure F-(Ca^{2+}/Mg^{2+})-actin (0.086) (Figure 1 and Table 1), suggesting that ATP hydrolysis induces additional rotational motions in these Ca^{2+}-containing filaments.

The anisotropy of F-(Ca^{2+}/Mg^{2+})-actin during steady-state ATP hydrolysis was measured at several S1:actin ratios between 0 and 1 (Figure 1). An excess of ATP (25 mM) was used to ensure that the complex remained in active hydrolysis during the time required to collect polarization measurements of sufficient signal:noise ratio to ensure accuracy. A previous study (*18*) demonstrated that the anisotropy of actoS1 during ATP hydrolysis is constant over a range from 5 to 20 mM ATP; variations in ATP concentra-

Table 1: Steady-State Phosphorescence Anisotropy and Lifetime of F-Actin

cation	S1:actin	[KCl], mM	[ATP], mM	phalloidin	anisotropy[a]	lifetime,[a] μs
Ca^{2+}/Mg^{2+}	0	100	0	−	0.084 ± 0.002	290 ± 3
	1	100	0	−	0.132 ± 0.003	369 ± 7
	1	100	20	−	0.065 ± 0.004	292 ± 4
	0	100	0	+	0.102 ± 0.006	276 ± 4
	1	100	0	+	0.137 ± 0.005	358 ± 3
	1	100	10	+	0.077 ± 0.005	289 ± 2
	1	100	20	+	0.073 ± 0.004	−
	0	150	0	−	0.087 ± 0.003	300 ± 4
	1	150	0	−	0.133 ± 0.003	387 ± 3
	1	150	20	−	0.063 ± 0.003	299 ± 3
Ca^{2+}	0	0	0	−	0.082 ± 0.002	334 ± 8
	1	0	0	−	0.137 ± 0.003	385 ± 6
	1	0	10	−	0.071 ± 0.005	−
	1	0	20	−	0.067 ± 0.003	336 ± 3
	0	100	0	−	0.083 ± 0.002	306 ± 5
	1	100	0	−	0.136 ± 0.004	379 ± 5
	1	100	20	−	0.069 ± 0.006	302 ± 1
Mg^{2+}	0	0	0	−	0.065 ± 0.003	306 ± 7
	1	0	0	−	0.137 ± 0.006	388 ± 5
	1	0	10	−	0.063 ± 0.004	−
	1	0	25	−	0.063 ± 0.003	288 ± 3
	0	100	0	−	0.066 ± 0.003	261 ± 4
	1	100	0	−	0.138 ± 0.005	387 ± 2
	1	100	10	−	0.063 ± 0.003	−
	1	100	20	−	0.064 ± 0.004	258 ± 1
	0	100	0	+	0.080 ± 0.005	271 ± 5
	1	100	0	+	0.143 ± 0.005	362 ± 5
	1	100	20	+	0.071 ± 0.002	262 ± 4
	0	150	0	−	0.068 ± 0.005	264 ± 5
	1	150	0	−	0.141 ± 0.002	391 ± 3
	1	150	20	−	0.066 ± 0.004	262 ± 4

[a] Mean ± standard deviation of at least three replicates.

tion from 10 to 25 mM had no effect on the measured anisotropy in the current study (Table 1). The addition of ATP to a subsaturated acto−S1 complex (S1:actin = 0.2) also caused a decrease in the anisotropy of F-(Ca^{2+}/Mg^{2+})-actin to a value (0.067) lower than that seen in pure F-(Ca^{2+}/Mg^{2+})-actin and essentially identical to that obtained for the 1:1 complex during ATP hydrolysis (0.065). Similar results were observed for other actoS1 complexes at higher S1:actin ratios; only the sample with an S1:actin ratio of 0.1 did not display a low anisotropy value during ATP hydrolysis (Figure 1). In all cases, the phosphorescence lifetime was essentially identical for pure F-actin and for actomyosin filaments during ATP hydrolysis (Table 1). These results suggest that ATP hydrolysis by a relatively small number of myosin heads bound to actin can induce rotational motions in F-(Ca^{2+}/Mg^{2+})-actin. Centrifugation experiments indicated that only about 10% of S1 is bound to F-actin during active hydrolysis at S1:actin ratios of 1:1, 1:4, and 1:10.

Anisotropy of F-Mg^{2+}-ActoS1 Complexes in Rigor and during Steady-State ATP Hydrolysis. Similar studies were carried out on actin filaments polymerized in the presence of Mg^{2+}-FB and thus containing Mg^{2+} as the tightly bound cation (F-Mg^{2+}-actin). The phosphorescence anisotropy of F-Mg^{2+}-actin also increased nonlinearly with the S1:actin ratio (Figure 2). Although the phosphorescence lifetime of the erythrosin probe increased with the S1:actin ratio (data for S1:actin ratios of 0 and 1 are listed in Table 1), the observed increase in the anisotropy cannot be due to such increases (*17*, *18*) since an increase in lifetime in the absence of any other dynamic changes would decrease the steady-state anisotropy (*33*). As for the F-(Ca^{2+}/Mg^{2+})-actin filaments, the increase in the anisotropy of F-Mg^{2+}-actin upon binding S1 thus reflected an overall increase in the rigidity of the actin filament.

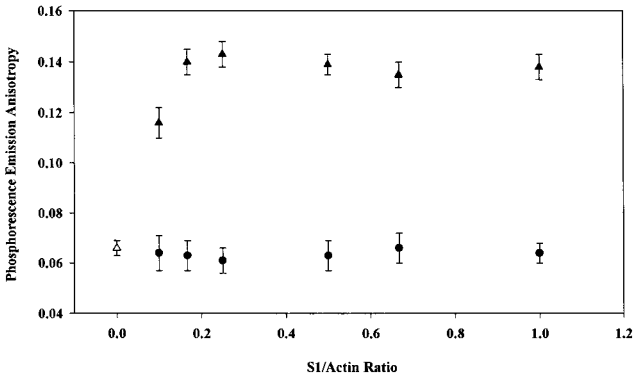

FIGURE 2: Steady-state phosphorescence emission anisotropy of F-Mg^{2+}-actin (△) and of 1:1 F-Mg^{2+}-actoS1 complexes in rigor (▲) and during steady-state ATP hydrolysis (●) in the presence of 25 mM ATP. All measurements were made at 20 °C in buffer Mg^{2+}-FB containing 100 mM KCl.

The anisotropy of F-Mg^{2+}-actin saturated with S1 (0.138) was similar to that of the F-(Ca^{2+}/Mg^{2+})-actoS1 complex (0.132). Because the probes have similar lifetimes in these two complexes (Table 1), the rotational motions taking place in these two types of actoS1 filaments are similar. Although the lower anisotropy of F-Mg^{2+}-actin indicates that it is more flexible than F-(Ca^{2+}/Mg^{2+})-actin (*12*, *21*), rigor binding of S1 to each type of filament apparently induced a unique rigid state that is independent of the type of tightly bound divalent cation (Ca^{2+} or Mg^{2+}). The increase in the anisotropy upon binding S1, however, was much greater for F-Mg^{2+}-actin (from 0.069 to 0.138 or a 100% increase) than for F-(Ca^{2+}/

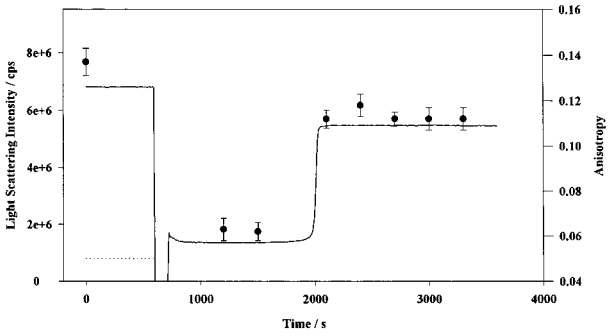

FIGURE 3: Light scattering from actoS1 (—) and pure F-actin (···) and steady-state phosphorescence anisotropy of actoS1 (●) as a function of time before and after addition of ATP. All samples included erythrosin-labeled F-Mg^{2+}-actin; S1 was added at a ratio of 1 S1/actin. ATP (sufficient to make the solution 10 mM) was added to the solutions at the 600 s time point. All measurements were made at 20 °C in buffer Mg^{2+}-FB without KCl. See Materials and Methods for further details.

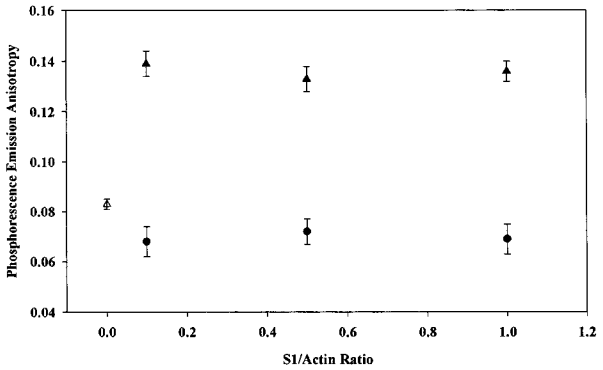

FIGURE 4: Steady-state phosphorescence emission anisotropy of F-Ca^{2+}-actin (△) and of 1:1 F-Ca^{2+}-actoS1 complexes in rigor (▲) and during steady-state ATP hydrolysis (●) in the presence of 25 mM ATP plus 5 mM Mg^{2+}. All measurements were made at 20 °C in Ca^{2+}-FB buffer containing 100 mM KCl.

Mg^{2+})-actin (from 0.085 to 0.132 or a 55% increase). This indicates that S1 binding had a larger effect on the rigidity of F-actin containing tightly bound Mg^{2+} than on filaments containing tightly bound Ca^{2+}.

Upon addition of ATP to the 1:1 actoS1 complex, the phosphorescence anisotropy of F-Mg^{2+}-actin dropped to a value (0.064) similar to that seen in the pure F-Mg^{2+}-actin filament (0.066); the phosphorescence lifetimes were nearly identical in the two states (Table 1). The time course of this decrease in anisotropy was coincident with a decrease in light scattering (Figure 3) that reflected dissociation of S1 from F-Mg^{2+}-actin upon binding ATP. Upon addition of ATP (10 mM) to the 1:1 actoS1 complex, the intensity of light scattering decreased to a value very close to that of F-Mg^{2+}-actin alone. Assuming that the magnitude of the scattering intensity is linear with the concentration of actoS1, about 10% of the S1 remained associated with the filament during steady-state ATP hydrolysis. After depletion of ATP, both the light scattering intensity and the phosphorescence anisotropy increased to values that were slightly lower than the initial values measured in the rigor complexes; the lower values reflected the effect of 10 mM ADP+P_i on the structure of the complex (*18*).

Across all S1:actin ratios from 0.1 to 1.0 (Figure 2), the anisotropy of F-Mg^{2+}-actin during ATP hydrolysis dropped to approximately the same value (~0.065), indicating that the rotational motions observed in Mg^{2+}-F-actin during ATP hydrolysis were similar at these divergent S1:actin ratios. These data indicate that ATP hydrolysis on S1 did not induce additional rotational motions in Mg^{2+}-containing F-actin.

Anisotropy of F-Ca^{2+}-ActoS1 Complexes in Rigor and during Steady-State ATP Hydrolysis. Our previous study (*21*) established that F-Ca^{2+}-actin (polymerized from G-Ca^{2+}-actin in the presence of Ca^{2+}-FB) has similar rotational flexibility to F-(Ca^{2+}/Mg^{2+})-actin under a variety of solution conditions. Upon titration with S1, the anisotropy of F-Ca^{2+}-actin in a 1:1 acto:S1 complex increased from 0.083 to 0.136, a rigor value quite similar to that obtained for 1:1 S1 complexes with F-(Ca^{2+}/Mg^{2+})-actin and F-Mg^{2+}-actin (Table 1). Upon addition of ATP to the rigor F-Ca^{2+}-actoS1 (1:1) complex, the anisotropy dropped to a value (0.069) significantly lower than that of F-Ca^{2+}-actin itself (0.083); light scattering measurements as a function of time after addition of 10 mM ATP (data not shown) displayed a time course quite similar to that depicted in Figure 3. Upon addition of ATP to the F-Ca^{2+}-actoS1 complexes (Figure 4), the anisotropy dropped below the pure filament value at all S1:actin ratios in a manner essentially identical to that seen in F-(Ca^{2+}/Mg^{2+})-actin. ATP hydrolysis by attached S1 thus decreased the anisotropy of both F-Ca^{2+}-actin and F-(Ca^{2+}/Mg^{2+})-actin filaments in a similar manner. Since both F-(Ca^{2+}/Mg^{2+})-actin and F-Ca^{2+}-actin are Ca^{2+}-containing actin filaments (*18*, *45*), comparison of these data with those collected for F-Mg^{2+}-actin indicate that ATP hydrolysis by S1 induced rotational motions in Ca^{2+}-containing F-actin but not in Mg^{2+}-containing F-actin.

Effect of Ionic Strength on the Anisotropy of Actin Filaments. Variations in the ionic strength of the buffer brought about by changes in the concentration of KCl over the range from 0 to 150 mM had no apparent effect on the anisotropy of actin filaments containing either tightly bound Ca^{2+} or Mg^{2+} (Table 1). (Note that the data in Figures 1, 2, and 4 were all collected in buffer FB containing 100 mM KCl.) The rotational dynamics of F-actin and of actoS1 either in rigor or during ATP hydrolysis were thus largely unaffected by ionic strength despite the known influence of salt concentration on the strength of the S1−actin interaction (*38*−*40*).

Anisotropy of Phalloidin-Stabilized ActoS1 Filaments. The fungal toxin phalloidin binds to and stabilizes the actin filament by strengthening the bonds both across and along the two-start helix (*23*, *41*). Phalloidin also increases the phosphorescence anisotropy and thus the rigidity of F-actin irrespective of the type of tightly bound divalent cation (*21*). The phosphorescence emission anisotropy of F-(Ca^{2+}/Mg^{2+})-actin increased from 0.102 to 0.137 (34%) upon S1 binding in the presence of phalloidin (Table 1) while it increased from 0.084 to 0.132 (57%) upon binding S1 in its absence. Since phalloidin binding had no influence on the probe lifetime (Table 1), S1 binding thus had a smaller effect on the rigidity of phalloidin-stabilized F-actin than on unstabilized F-actin. Phalloidin binding increased the anisotropy of actoS1 only slightly if at all; since the lifetime was unaffected, the rigidity of the actoS1 complex, in contrast to pure F-actin, was largely unaffected by phalloidin. Upon addition of ATP to the phalloidin-stabilized F-(Ca^{2+}/Mg^{2+})-actin complex with S1, the anisotropy dropped to a value

(0.073) lower than that seen in the pure phalloidin-stabilized filaments (0.102) (Table 1). ATP hydrolysis by S1 thus also induced rotational motions in phalloidin-stabilized Ca^{2+}-containing filaments.

S1 binding to phalloidin-stabilized F-Mg^{2+}-actin caused an approximately 80% increase in the anisotropy (from 0.080 to 0.143) (Table 1). This increase was significantly less than the 110% increase seen in the absence of phalloidin (Table 1) because, while the anisotropy of F-Mg^{2+}-actin was increased significantly by phalloidin, the anisotropy of actoS1 filaments was increased only slightly by phalloidin. Upon addition of ATP to the 1:1 phalloidin-stabilized F-Mg^{2+}-actoS1 complex, the anisotropy decreased to a value (0.071) below that seen in the pure phalloidin-stabilized F-Mg^{2+}-actin filament (0.080). ATP hydrolysis by S1 thus induced rotational motions in F-Mg^{2+}-actin in the presence of phalloidin but not in its absence.

DISCUSSION

Torsional Dynamics of ActoS1 Complexes in Rigor. This study demonstrates that rigor S1 binding induced a cooperative decrease in the rotational motions of F-actin irrespective of the type of tightly bound divalent cation. The fully saturated actoS1 complexes had similar anisotropy values and phosphorescence lifetimes (Table 1) independent of the type of cation bound or the presence of phalloidin. F-Mg^{2+}-actin and F-(Ca^{2+}/Mg^{2+})-actin + phalloidin, for example, whose anisotropy values differ by over 50% (0.066 and 0.102, respectively), had nearly identical anisotropy values in a 1:1 complex with S1 (0.138 and 0.137, respectively). Since the average lifetimes of the probe in these two complexes were quite similar (387 and 358 μs, respectively), their rotational dynamics must also be quite similar. Similar anisotropy and lifetime values in the other actoS1 filaments indicate that S1 induces a similar dynamic state in F-actin regardless of the initial flexibility of the filament.

The exact mechanism by which this occurs is not yet known; however, the effect cannot be explained by a simple increase in the mass of the filament caused by S1 binding (*35*). The nonlinear increase in the anisotropy of F-actin upon titration with bound rigor heads certainly reflects cooperative changes induced in F-actin (*42*). Prochniewicz and Thomas (*20*), based on time-resolved phosphorescence decay measurements of erythrosin-labeled actin, have proposed that the increase in filament rigidity results from structural changes at the myosin binding sites on F-actin. An exact molecular explanation, however, awaits further details about the structure of actin in the myosin complex. Whatever the mechanism, such binding appears to effectively immobilize F-actin rotational and torsional motions on the microsecond time scale since the steady-state anisotropy of actoS1 (0.13−0.14) is only marginally lower than the anisotropy (0.15−0.16) observed for F-actin immobilized in viscous solution or within a gel matrix (*32*).

Our results on the effect of cations on the microsecond rotational motions of F-actin differ from dynamic results obtained on the nanosecond time scale (*43*). Fluorescence anisotropy measurements of *N*-(iodoacetyl)-*N*′-(5-sulfo-1-naphthyl)ethylenediamine covalently attached at Cys374 of actin indicate that rigor binding of myosin heads (HMM or S1) induced a cooperative decrease in actin rotational mobility in the presence of Ca^{2+} yet increased actin mobility in the presence of Mg^{2+}. This discrepancy with our results may have its basis in the different physical origins of motions detected on the two time scales: nanosecond fluorescence measurements sense local, segmental motions of G-actin whereas microsecond phosphorescence measurements detect larger scale, perhaps cooperative, motions of F-actin (*19*).

Torsional Dynamics of ActoS1 Complexes during ATP Hydrolysis. In a previous study (*21*), we demonstrated that the type of divalent cation bound at the high-affinity site of F-actin modulated the microsecond rotational motions of the actin filament; filaments polymerized with Mg^{2+} exhibit greater rotational flexibility on the microsecond time scale. The current study expands the dynamic repertoire of the actin filament to include differential dynamic response to forces generated during ATP hydrolysis by attached myosin heads. Not only is F-actin able to respond to such forces by an increase in rotational motions, but also the extent of this response is sensitive to the type of divalent cation bound at the nucleotide binding site and to the binding of phalloidin, a fungal toxin which stabilizes the filament structure. Uncertainty remains, however, about the precise molecular origins of the differences observed by the phosphorescence anisotropy measurements.

The differences in rotational dynamics between Mg^{2+}- and Ca^{2+}-containing filaments may be interpreted in two distinctly different ways. On one hand, the additional flexibility in Mg^{2+} filaments or in Ca^{2+} filaments during ATP hydrolysis may reflect additional domain motions in individual actin monomers under those conditions. Kalbitzer and colleagues (*46*), for example, have shown that exchange of Mg^{2+} for Ca^{2+} increases the mobility (narrows the ^{1}H NMR line width) of a number of residues in F-actin. ATP hydrolysis by S1 may have a similar effect on some domain in Ca^{2+} F-actin or in Mg^{2+} F-actin in the presence of phalloidin. On the other hand, the additional flexibility in Mg^{2+} filaments or in Ca^{2+} filaments during ATP hydrolysis may reflect differences in the large-scale rotational motions of the filament. This is the interpretation argued by us in previous steady-state studies of F-actin dynamics (*18, 21*).

Although our results do not resolve this controversy, several lines of evidence lead us to conclude that changes in filament torsional flexibility provide the best interpretation of the changes in phosphorescence anisotropy reported here [these and other arguments are developed more fully elsewhere (*18, 19, 21*)]. First, since the study of Kalbitzer and colleagues (*46*) indicated that Cys374 (the site of attachment of the erythrosin probe used herein) actually remains immobile in the presence of either Ca^{2+} or Mg^{2+}, domain motions at this site thus remain speculative. Second, the time constants determined from anisotropy measurements are sufficiently long to argue for the involvement of large-scale protein motion involving many monomers rather than localized motion within a monomer (*19*). Long axis torsional motion is the only possible large-scale rotational motion within an entangled filament network such as F-actin (*47*). Third, the large dynamic effect of ATP hydrolysis at S1:actin ratios as low as 0.2 indicates that the motion of the probe is affected by events occurring at distant actin sites; this suggests that the anisotropy decreases due to cooperative motions involving many actin monomers. The dynamic response to S1 binding provides additional (albeit less

Table 2: Steady-State Phosphorescence Emission Anisotropy of Actin Filaments Arranged in Order of Increasing Torsional Rigidity

state	Mg^{2+}-actin	phalloidin-Mg^{2+}-actin	Ca^{2+}-actin	(Ca^{2+}/Mg^{2+})-actin	phalloidin-(Ca^{2+}/Mg^{2+})-actin
actoS1 (1:1)	0.138	0.143	0.136	0.132	0.137
F-actin	0.066	0.080	0.083	0.086	0.102
actoS1+ATP	0.064	0.071	0.069	0.065	0.073
difference[a]	0.002	0.009	0.014	0.021	0.029

[a] The difference between the filament anisotropy of pure F-actin and that of actoS1 during ATP hydrolysis.

dramatic) evidence for cooperative interactions among monomers.

In the context of a global filament motion model, the phosphorescence anisotropy provides an indirect measure of the torsional rigidity of the actin filament (*20, 33*). The extent of the torsional response of actin to ATP hydrolysis can thus be estimated by the extent to which the steady-state anisotropy decreases below its value in pure F-actin. [Since the probe lifetime is essentially identical in the two states (Table 1), this difference is an accurate reflection of any increase in torsional motions; however, the complex functional relation connecting steady-state anisotropy to torsional rigidity (*33*) precludes any simple equation of the two beyond the requirement that an increase in anisotropy reflects an increase in torsional rigidity.] These differences are listed in Table 2 in order of the increasing anisotropy (in our interpretation, in order of increasing torsional rigidity) of the pure F-actin. The magnitude of the decrease in anisotropy during ATP hydrolysis is proportional to the anisotropy of the pure filament. This suggests that more rigid filaments undergo more extensive torsional motions during ATP hydrolysis. We propose that the differential response of Mg^{2+}- and Ca^{2+}-containing filaments to ATP hydrolysis is actually due to the effect of these cations on the torsional rigidity of the actin filament (*21*).

A crucial finding supporting this interpretation is the effect of phalloidin on the torsional response of F-Mg^{2+}-actin to ATP hydrolysis. Mg^{2+}-containing filaments are dynamically unresponsive to hydrolysis on the probe time scale (about 300 μs) whereas in the presence of phalloidin they become so. This demonstrates that the dynamic insensitivity is not a property intrinsic to the structure of the Mg^{2+}-containing filaments. The correlation summarized in Table 2 suggests that phalloidin binding induces this dynamic sensitivity by increasing the torsional rigidity of the filament.

How might filament rigidity mediate filament response to ATP hydrolysis? In essence, an increase in rigidity may increase the cooperativity of the filament response to any applied perturbation. In our interpretation, the decrease in phosphorescence anisotropy that occurs during ATP hydrolysis is a global dynamic response to a local structural event. As mentioned above, and argued in more detail in our earlier study of induced motions in actin (*18*), our anisotropy measurement is sensitive to large-scale global rotational motions of the filament occurring in the filament during hydrolysis. Despite this, the anisotropy was found to decrease during ATP hydrolysis even at low S1 saturation (S1:actin = 0.2) or at high saturation at high ionic strength where the S1 binding is weaker. Since the fraction of heads attached to F-(Ca^{2+}/Mg^{2+})-actin during hydrolysis was estimated at only 10% even at S1:actin ratios of 1:10, then S1 can apparently induce large-scale torsional motions in F-actin when only about 1−2% of the binding sites have S1 bound. This is a remarkable finding that demands further confirmation.

The extent to which a torsional perturbation (twisting motion) at a single actin site is propagated along the filament depends on the torsional rigidity of the filament, that is, depends on the extent of physical coupling among actin monomers in the filament. A torsionally flexible filament would be able to relax a torsional perturbation over a short distance while a more rigid filament would require longer distances. (Contrast, if you will, our ability to manipulate individual cooked and uncooked spaghetti noodles.) Mg^{2+} filaments are not rigid enough to propagate any local torsional motions induced by S1 over a sufficient distance to be detectable by the phosphorescence anisotropy measurement. Phalloidin binding, however, increases the filament rigidity enough to make such perturbations detectable. Ca^{2+} filaments, however, are sufficiently rigid to propagate global rotational motions that are detectable by the anisotropy; phalloidin binding to these filaments merely increases the physical extent of the torsional response by increasing the torsional rigidity. Orlova and Egelman (36) have provided structural evidence indicating that F-Mg^{2+}-actin with phalloidin bound exhibits structural features similar to that of F-Ca^{2+}-actin. Differences in the connectivity between the actin monomers either along or between the two long-pitch helical strands in the actin filament provide a reasonable structural explanation of our dynamic results (*21*).

Our finding that myosin heads can induce rotational motions in F-actin even at low saturation would suggest that the torque component of the sliding force exerted by S1 against F-actin is quite large; however, Suzuki et al. (*28*) estimated that this torque is only 10% of the total sliding force. Since it is difficult to imagine how such a small torque exerted by so few bound heads could generate the extensive motions observed in this and our previous study (*18*), such an explanation for the origins of induced torsional motions remains problematic.

Egelman and Orlova (*29*) have suggested that myosin binding to F-actin induces torsional strain in the filament. Electron microscopy studies by Menetret et al. (*45*) provide images consistent with this suggestion. It is thus possible that the torsional motions induced by ATP hydrolysis result from torsional relaxation of this strain upon release of bound S1 following binding of ATP. Once again the physical extent of any cooperative torsional motions taking place in the actin filament that result from torsional relaxation would depend on the rigidity (structural connectivity among the monomers) of the actin filament. Such an explanation could be tested by measurements of the torsional motion of actoS1 complexes following rapid mixing with ATP or perhaps AMP-PNP: the coordinated release of bound heads should induce a large decrease in the filament anisotropy even, perhaps, in relatively flexible filaments such as F-Mg^{2+}-actin. We are not aware, however, of any stopped-flow measurements of phosphorescence anisotropy.

REFERENCES

1. Oosawa, F., and Asakawa, S. (1975) *Thermodynamics of the Polymerization of Proteins*, Academic Press, Sydney.

2. Korn, E. D., Carlier, M.-F., and Pantaloni, D. (1987) *Science 238*, 638−644.
3. Carlier, M.-F. (1990) *Adv. Biophys. 26*, 51−73.
4. McLaughlin, P. J., Gooch, J. T., Mannherz, H.-G., and Weeds, A. G. (1993) *Nature 364*, 685−692.
5. Fujime, S., and Ishiwata, S. (1971) *J. Mol. Biol. 62*, 251−265.
6. Ishiwata, S., and Fujime, S. (1972*) J. Mol. Biol. 68*, 511−522.
7. Janmey, P. A., Hvidt, S., Oster, G. F., Lamb, J., Stossel, T. P., and Hartwig, J. H. (1990) *Nature 347*, 95−99.
8. Yanagida, T., Nakase, M., Nishiyama, K., and Oosawa, F. (1984) *Nature 307*, 58−60.
9. Isambert, H., Venier, P., Maggs, A. C., Fattoum, A., Kassab, R., Pantaloni, D., and Carlier, M.-F. (1995) *J. Biol. Sci. 270*, 11437−11444.
10. Nishizaka, T., Yagi, T., Tananka, Y. and Ishiwata, S. (1993) *Nature 361*, 269−271.
11. Kas, J., Strey, H., and Sackmann, E. (1994) *Nature 368*, 226−229.
12. Yasuda, R., Miyata, H., and Kinosita, K., Jr. (1996) *J. Mol. Biol. 263*, 227−236.
13. Muller, O., Gaub, H. E., and Sackmann, E. (1991) *Macromolecules 24*, 3111−3120.
14. Janmey, P. A. (1991) *Curr. Opin. Cell Biol. 2*, 4−11.
15. Zieman, F., Radler, J., and Sackmann, E. (1994) *Biophys. J. 66*, 2210−2216.
16. Yoshimura, H., Nishio, T., Mihashi, K., Kinosita, K., and Ikegami, A. (1984) *J. Mol. Biol. 132*, 257−273.
17. Ng, C.-M., and Ludescher, R. D. (1994) *Proc. SPIE 2137*, 448−455.
18. Ng, C.-M., and Ludescher, R. D. (1994) *Biochemistry 33*, 9098−9104.
19. Prochniewicz, E., Zhang, Q., Howard, E., and Thomas, D. (1996) *J. Mol. Biol. 255*, 446−457.
20. Prochniewicz, E., and Thomas, D. (1997) *Biochemistry 36*, 12845−12853.
21. Rebello, C. A., and Ludescher, R. D. (1998) *Biochemistry 37*, 14529−14538.
22. Holmes, K. C., Popp, D., Gebhard, W., and Kabsch, W. (1990) *Nature 347*, 37−44.
23. Lorenz, M., Popp, D., and Holmes, K. C. (1993) *J. Mol. Biol. 234*, 826−836.
24. Kojima, H., Ishijima, A., and Yanagida, T. (1994) *Proc. Natl. Acad. Sci. U.S.A. 91*, 12962−12966.
25. Wakabayashi, K., Sugimoto, Y., Tanaka, H., Ueno, Y., Takezawa, Y., and Amemiya, Y. (1994) *Biophys. J. 67*, 2422−2435.
26. Huxley, H. E., Stewart, A., Sosa, H., and Irving, T. (1994) *Biophys. J. 67*, 2411−2421.
27. Tanaka, Y., Ishijima, A., and Ishiwata, S. (1992) *Biochim. Biophys. Acta 1159*, 94−98.
28. Suzuki, N., Miyata, H., Ishiwata, S., and Kinosita, K. (1996) *Biophys. J. 70*, 401−414.
29. Orlova, A., and Egelman, E. H. (1997) *J. Mol. Biol. 265*, 469−474.
30. Orlova, A., and Egelman, E. H. (1995) *J. Mol. Biol. 245*, 582−597.
31. Orlova, A., and Egelman, E. H. (1995) *J. Mol. Biol. 245*, 598−607.
32. Ludescher, R. D., and Liu, Z. (1993) *Photochem. Photobiol. 58*, 858−866.
33. Ludescher, R. D., and Ludescher, W. H. (1993) *Photochem. Photobiol. 58*, 881−883.
34. Pardee, J., and Spudich, J. (1982) *Methods Enzymol. 65*, 164−181.
35. Thomas, D. D., Seidel, J. C., and Gergely, J. (1979) *J. Mol. Biol. 132*, 257−273.
36. Orlova, A., and Egelman, E. (1993) *J. Mol. Biol. 232*, 334−341.
37. Horie, T., and Vanderkooi, J. (1981) *Biochim. Biophys. Acta 670*, 294−297.
38. Eisenberg, E., and Moos, C. (1968) *Biochemistry 7*, 1486−1489.
39. Rizzino, A. A., Barouch, W. W., Eisenberg, E., and Moos, C. (1970) *Biochemistry 9*, 2402−2408.
40. Greene, L. E., Sellers, J. R., Eisenberg, E., and Adelstein, R. S. (1983) *Biochemistry 22*, 530−539.
41. Bremer, A., Millonig, R. C., Sutterlin, R., Engel, A., Pollard, T. D., and Aebi, U. (1991) *J. Cell Biol. 115*, 689−703.
42. Prochniewicz, E., Katayama, E., Yanagida, T., and Thomas, D. D. (1993) *Biophys. J. 65*, 113−123.
43. Miki, M., Wahl, P., and Auchet, J.-C. (1982) *Biochemistry 21*, 3661−3665.
44. Menetret, J.-F., Hofmann, W., Schroder, R. R., Rapp, G., and Goody, R. S. (1991) *J. Mol. Biol. 219*, 139−144.
45. Estes, J. E., Selden, L. A., Kinosian, H. J., and Gersham, L. C. (1992) *J. Muscle Res. Cell Motil. 13*, 272−284.
46. Heintz, D., Kany, H., and Kalbitzer, H. R. (1996) *Biochemistry 35*, 12686−12693.
47. Kas, J., Strey, H., and Sackmann, E. (1994) *Nature 368*, 226−229.

BI990348A